

1-1-2003

Measurement of the polarized structure function $\sigma_{LT'}$ for $p(\vec{e}, e'p)\pi^0$ in the $\Delta(1232)$ resonance region

K. Joo

Angela Biselli

Fairfield University, abiselli@fairfield.edu

CLAS Collaboration

Copyright American Physical Society Publisher final version available at <http://prc.aps.org/pdf/PRC/v68/i3/e032201>

Peer Reviewed

Repository Citation

Joo, K.; Biselli, Angela; and CLAS Collaboration, "Measurement of the polarized structure function $\sigma_{LT'}$ for $p(\vec{e}, e'p)\pi^0$ in the $\Delta(1232)$ resonance region" (2003). *Physics Faculty Publications*. 97.
<http://digitalcommons.fairfield.edu/physics-facultypubs/97>

Published Citation

K. Joo et al. [CLAS Collaboration], "Measurement of the polarized structure function $\sigma_{LT'}$ for $p(\vec{e}, e'p)\pi^0$ in the $\Delta(1232)$ resonance region", *Physical Review C* 68.3 (2003) DOI: 10.1103/PhysRevC.68.032201

This Article is brought to you for free and open access by the Physics Department at DigitalCommons@Fairfield. It has been accepted for inclusion in Physics Faculty Publications by an authorized administrator of DigitalCommons@Fairfield. For more information, please contact digitalcommons@fairfield.edu.

Measurement of the polarized structure function $\sigma_{LT'}$ for $p(\vec{e}, e'p)\pi^0$ in the $\Delta(1232)$ resonance region

K. Joo,^{1,2,3} L. C. Smith,² V. D. Burkert,³ R. Minehart,² G. Adams,³¹ P. Ambrozewicz,¹² E. Anciant,⁵ M. Anghinolfi,¹⁷ B. Asavapibhop,²⁴ G. Audit,⁵ T. Auger,⁵ H. Avakian,³ H. Bagdasaryan,²⁸ J. P. Ball,⁴ S. Barrow,¹³ M. Battaglieri,¹⁷ K. Beard,²¹ M. Bektasoglu,²⁷ M. Bellis,³¹ N. Benmouna,¹⁴ N. Bianchi,¹⁶ A. S. Biselli,⁷ S. Boiarinov,²⁰ S. Bouchigny,¹⁸ R. Bradford,⁷ D. Branford,¹¹ W. J. Briscoe,¹⁴ W. K. Brooks,³ C. Butuceanu,³⁸ J. R. Calarco,²⁵ D. S. Carman,²⁷ B. Carnahan,⁸ C. Cetina,¹⁴ L. Ciciani,²⁸ P. L. Cole,³⁵ A. Coleman,³⁸ D. Cords,³ P. Corvisiero,¹⁷ D. Crabb,² H. Crannell,⁸ J. P. Cummings,³¹ E. DeSanctis,¹⁶ R. De Vita,¹⁷ P. V. Degtyarenko,³ H. Denizli,²⁹ L. Dennis,¹³ K. V. Dharmawardane,²⁸ K. S. Dhuga,¹⁴ C. Djalali,³⁴ G. E. Dodge,²⁸ D. Doughty,⁹ P. Dragovitsch,¹³ M. Dugger,⁴ S. Dytman,²⁹ O. P. Dzyubak,³⁴ M. Eckhause,³⁸ H. Egiyan,³ K. S. Egiyan,³⁹ L. Elouadrhiri,⁹ A. Empl,³¹ P. Eugenio,¹³ R. Fatemi,² R. J. Feuerbach,⁷ J. Ficenec,³⁷ T. A. Forest,²⁸ H. Funsten,³⁸ S. J. Gaff,¹⁰ G. Gavalian,²⁵ S. Gilad,²³ G. P. Gilfoyle,³³ K. L. Giovanetti,²¹ P. Girard,³⁴ C. I. O. Gordon,¹⁵ K. Griffioen,³⁸ M. Guidal,¹⁸ M. Guillo,³⁴ L. Guo,³ V. Gyurjyan,³ C. Hadjidakis,¹⁸ R. S. Hakobyan,⁸ J. Hardie,⁹ D. Heddle,⁹ P. Heimberg,¹⁴ F. W. Hersman,²⁵ K. Hicks,²⁷ R. S. Hicks,²⁴ M. Holtrop,²⁵ J. Hu,³¹ C. E. Hyde-Wright,²⁸ Y. Ilieva,¹⁴ M. M. Ito,³ D. Jenkins,³⁷ J. H. Kelley,¹⁰ M. Khandaker,²⁶ K. Y. Kim,²⁹ K. Kim,²² W. Kim,²² A. Klein,²⁸ F. J. Klein,^{3,8} A. V. Klimentenko,²⁸ M. Klusman,³¹ M. Kossov,²⁰ L. H. Kramer,¹² Y. Kuang,³⁸ S. E. Kuhn,²⁸ J. Kuhn,⁷ J. Lachniet,⁷ J. M. Laget,⁵ D. Lawrence,²⁴ Ji Li,³¹ A. C. S. Lima,¹⁴ K. Lukashin,^{37,8} J. J. Manak,³ C. Marchand,⁵ S. McAleer,¹³ J. W. C. McNabb,⁷ B. A. Mecking,³ S. Mehrabyan,²⁹ J. J. Melone,¹⁵ M. D. Mestayer,³ C. A. Meyer,⁷ K. Mikhailov,²⁰ M. Mirzazita,¹⁶ R. Miskimen,²⁴ L. Morand,⁵ S. A. Morrow,⁵ M. U. Mozer,²⁷ V. Muccifora,¹⁶ J. Mueller,²⁹ L. Y. Murphy,¹⁴ G. S. Mutchler,³² J. Napolitano,³¹ R. Nasseripour,¹² S. O. Nelson,¹⁰ S. Niccolai,¹⁴ G. Niculescu,²⁷ I. Niculescu,²¹ B. B. Niczyporuk,³ R. A. Niyazov,²⁸ M. Nozar,³ G. V. O'Rielly,¹⁴ A. K. Opper,²⁷ M. Osipenko,¹⁷ K. Park,²² E. Pasyuk,⁴ G. Peterson,²⁴ S. A. Philips,¹⁴ N. Pivnyuk,²⁰ D. Pocanic,² O. Pogorelko,²⁰ E. Polli,¹⁶ S. Pozdniakov,²⁰ B. M. Preedom,³⁴ J. W. Price,⁶ Y. Prok,² D. Protopopescu,¹⁵ L. M. Qin,²⁸ B. A. Raue,¹² G. Riccardi,¹³ G. Ricco,¹⁷ M. Ripani,¹⁷ B. G. Ritchie,⁴ F. Ronchetti,¹⁶ P. Rossi,¹⁶ D. Rowntree,²³ P. D. Rubin,³³ F. Sabatié,⁵ K. Sabourov,¹⁰ C. Salgado,²⁶ J. P. Santoro,³⁷ V. Sapunenko,¹⁷ M. Sargsyan,¹² R. A. Schumacher,⁷ V. S. Serov,²⁰ Y. G. Sharabian,³⁹ J. Shaw,²⁴ S. Simionatto,¹⁴ A. V. Skabelin,²³ E. S. Smith,³ D. I. Sober,⁸ M. Spraker,¹⁰ A. Stavinsky,²⁰ S. Stepanyan,³⁹ P. Stoler,³¹ I. I. Strakovsky,¹⁴ S. Strauch,¹⁴ M. Taiuti,¹⁷ S. Taylor,³² D. J. Tedeschi,³⁴ U. Thoma,³ R. Thompson,²⁹ L. Todor,⁷ C. Tur,³⁴ M. Ungaro,³¹ M. F. Vineyard,³⁶ A. V. Vlassov,²⁰ K. Wang,² L. B. Weinstein,²⁸ H. Weller,¹⁰ D. P. Weygand,³ C. S. Whisnant,³⁴ E. Wolin,³ M. H. Wood,³⁴ A. Yegneswaran,³ J. Yun,²⁸ J. Zhao,²³ and Z. Zhou²³

(CLAS Collaboration)

¹University of Connecticut, Storrs, Connecticut 06269, USA

²University of Virginia, Charlottesville, Virginia 22901, USA

³Thomas Jefferson National Accelerator Facility, Newport News, Virginia 23606, USA

⁴Arizona State University, Tempe, Arizona 85287-1504, USA

⁵CEA-Saclay, Service de Physique Nucléaire, F91191 Gif-sur-Yvette, Cedex, France

⁶University of California at Los Angeles, Los Angeles, California 90095-1547, USA

⁷Carnegie Mellon University, Pittsburgh, Pennsylvania 15213, USA

⁸Catholic University of America, Washington, DC 20064, USA

⁹Christopher Newport University, Newport News, Virginia 23606, USA

¹⁰Duke University, Durham, North Carolina 27708-0305, USA

¹¹Edinburgh University, Edinburgh EH9 3JZ, United Kingdom

¹²Florida International University, Miami, Florida 33199, USA

¹³Florida State University, Tallahassee, Florida 32306, USA

¹⁴The George Washington University, Washington, DC 20052, USA

¹⁵University of Glasgow, Glasgow G12 8QQ, United Kingdom

¹⁶INFN, Laboratori Nazionali di Frascati, Frascati, Italy

¹⁷INFN, Sezione di Genova, 16146 Genova, Italy

¹⁸Institut de Physique Nucleaire ORSAY, Orsay, France

¹⁹Institute für Strahlen und Kernphysik, Universität Bonn, Germany

²⁰Institute of Theoretical and Experimental Physics, Moscow 117259, Russia

²¹James Madison University, Harrisonburg, Virginia 22807, USA

²²Kungpook National University, Taegu 702-701, South Korea

²³Massachusetts Institute of Technology, Cambridge, Massachusetts 02139-4307, USA

²⁴University of Massachusetts, Amherst, Massachusetts 01003, USA

²⁵University of New Hampshire, Durham, New Hampshire 03824-3568, USA

²⁶Norfolk State University, Norfolk, Virginia 23504, USA

²⁷Ohio University, Athens, Ohio 45701, USA

²⁸Old Dominion University, Norfolk, Virginia 23529, USA

²⁹*University of Pittsburgh, Pittsburgh, Pennsylvania 15260, USA*³⁰*Universia' di Roma, III, 00146 Eom, Italy*³¹*Rensselaer Polytechnic Institute, Troy, New York 12180-3590, USA*³²*Rice University, Houston, Texas 77005-1892, USA*³³*University of Richmond, Richmond, Virginia 23173, USA*³⁴*University of South Carolina, Columbia, South Carolina 29208, USA*³⁵*University of Texas at El Paso, El Paso, Texas 79968, USA*³⁶*Union College, Schenectady, New York 12308, USA*³⁷*Virginia Polytechnic Institute and State University, Blacksburg, Virginia 24061-0435, USA*³⁸*College of William and Mary, Williamsburg, Virginia 23187-8795, USA*³⁹*Yerevan Physics Institute, 375036 Yerevan, Armenia*

(Received 22 January 2003; published 30 September 2003)

The polarized longitudinal-transverse structure function $\sigma_{LT'}$ has been measured in the $\Delta(1232)$ resonance region at $Q^2=0.40$ and 0.65 GeV². Data for the $p(\vec{e}, e' p)\pi^0$ reaction were taken at Jefferson Lab with the CEBAF large acceptance spectrometer (CLAS) using longitudinally polarized electrons at an energy of 1.515 GeV. For the first time a complete angular distribution was measured, permitting the separation of different nonresonant amplitudes using a partial wave analysis. Comparison with previous beam asymmetry measurements at MAMI indicate a deviation from the predicted Q^2 dependence of $\sigma_{LT'}$ using recent phenomenological models.

DOI: 10.1103/PhysRevC.68.0322XX

PACS number(s): 13.60.Le, 12.40.Nn, 13.40.Gp

The $\gamma^*p \rightarrow \Delta^+(1232)$ transition has long served as a benchmark for testing nucleon models. In the SU(6) symmetric quark model, this strong magnetic dipole excitation is described as originating from a single quark spin flip. Residual spin-dependent and tensor-type interactions between the quarks are needed to explain the $N-\Delta$ mass difference and the small quadrupole transition strength observed in partial wave analyses of experimental pion electroproduction data [1–3]. Understanding the origin of these residual interactions and their role in resonance formation and decay is a fundamental challenge for modern QCD-inspired hadronic models.

In particular, the dynamical effects of the pion cloud are predicted to strongly modify the electromagnetic couplings at sufficiently low Q^2 . Chiral-quark and bag models that incorporate pion couplings [4–7] generally describe the $\Delta(1232)$ photocoupling multipoles better than a purely quark/gluon framework [8,9]. Recent dynamical models derived from effective chiral Lagrangians explicitly treat pion multiple scattering [10,11] and predict strong modifications to both resonant and nonresonant amplitudes. The role of the pion cloud in electromagnetic interactions is also being studied using heavy baryon chiral perturbation theory [12] and unquenched lattice QCD [13].

Unfortunately, cross section measurements alone do not provide sufficient information to separate the $\Delta(1232)$ excitation reaction mechanisms from nonresonant backgrounds and the tails of higher-mass resonances. Single spin polarization observables, on the other hand, are directly sensitive to the interference between resonant and nonresonant processes and together with precise cross sections can provide powerful constraints to models.

In this Rapid Communication we report new measurements of the longitudinal-transverse polarized structure function $\sigma_{LT'}$ obtained in the $\Delta(1232)$ resonance region using the $p(\vec{e}, e' p)\pi^0$ reaction. Recent measurements of polariza-

tion observables [14–17] and unpolarized cross sections [2,18] for $Q^2 < 0.2$ GeV² show disagreement with some dynamical models near the $\Delta(1232)$ peak. However, so far only narrow angular and kinematic ranges have been studied, yielding few clues as to the origin of the discrepancy. The present experiment was performed at four-momentum transfers $Q^2=0.40$ and 0.65 GeV² and covers a range of invariant mass $W=1.1-1.3$ GeV with full angular coverage in $\cos\theta_\pi^*$ and ϕ_π^* in the $p\pi^0$ center of mass (c.m.).

The data were taken at the Thomas Jefferson National Accelerator Facility (Jefferson Lab) using a 1.515 GeV, 100% duty-cycle beam of longitudinally polarized electrons incident on liquid hydrogen target. The electron polarization was determined by frequent Møller polarimeter measurements to be $0.69 \pm 0.009(\text{stat}) \pm 0.013(\text{syst})$. Scattered electrons and protons were detected in the CLAS spectrometer [19]. Electron triggers were enabled through a hardware coincidence of the gas Cerenkov counters and the lead-scintillator electromagnetic calorimeters. Protons were identified using momentum reconstruction in the tracking system and time of flight from the target to the scintillators. Software fiducial cuts were used to exclude regions of nonuniform detector response. Kinematic corrections were applied to compensate for drift chamber misalignments. The $p\pi^0$ final state was identified by requiring the missing neutral to have a mass squared between -0.01 and 0.05 GeV². Background from elastic Bethe-Heitler radiation was suppressed to below 1% using a combination of cuts on missing mass and ϕ_π^* near $\phi_\pi^*=0^\circ$. Target window backgrounds were suppressed with cuts on the reconstructed $e'p$ target vertex.

In the one-photon-exchange approximation, the electroproduction cross section factorizes as follows:

$$\frac{d^5\sigma}{dE_{e'}d\Omega_{e'}d\Omega_\pi^*} = \Gamma_v \frac{d^2\sigma^h}{d\Omega_\pi^*}, \quad (1)$$

where Γ_v is the virtual photon flux and $d^2\sigma^h$ is the differential cross section for $\gamma^*p \rightarrow p\pi^0$ with electron beam helicity ($h = \pm 1$). For an unpolarized target, $d^2\sigma^h$ depends on the transverse (ϵ) and longitudinal (ϵ_L) polarization of the virtual photon through five structure functions: σ_T, σ_L , and their interference terms σ_{TT}, σ_{LT} , and $\sigma_{LT'}$:

$$\frac{d^2\sigma^h}{d\Omega_\pi^*} = \frac{p_\pi^*}{k_\gamma^*} [\sigma_0 + h\sqrt{2\epsilon_L(1-\epsilon)}\sigma_{LT'}\sin\theta_\pi^*\sin\phi_\pi^*],$$

$$\sigma_0 = \sigma_T + \epsilon_L\sigma_L + \epsilon\sigma_{TT}\sin^2\theta_\pi^*\cos 2\phi_\pi^* + \sqrt{2\epsilon_L(1+\epsilon)}\sigma_{LT}\sin\theta_\pi^*\cos\phi_\pi^*, \quad (2)$$

where $(p_\pi^*, \theta_\pi^*, \phi_\pi^*)$ are the π^0 c.m. momentum, polar, and azimuthal angles, $\epsilon = [1 + 2|\vec{q}|^2 \tan^2(\theta_e/2)/Q^2]^{-1}$, $\epsilon_L = (Q^2/|k^*|^2)\epsilon$, and k_γ^* and $|k^*|$ are the virtual photon c.m. momentum and equivalent energy.

The structure functions σ_{LT} and $\sigma_{LT'}$ determine the real and imaginary parts of bilinear products between longitudinal and transverse amplitudes:

$$\sigma_{LT}: \text{Re}(L^*T) = \text{Re}(L)\text{Re}(T) + \text{Im}(L)\text{Im}(T), \quad (3)$$

$$\sigma_{LT'}: \text{Im}(L^*T) = \text{Re}(L)\text{Im}(T) - \text{Im}(L)\text{Re}(T). \quad (4)$$

Detection of a weak nonresonant background underlying the peak of the $\Delta(1232)$ can be enhanced through its interference in $\sigma_{LT'}$ with the strong transverse magnetic multipole $\text{Im}(M_{1+})$. Sensitivity to real backgrounds is suppressed in σ_{LT} due to the vanishing of $\text{Re}(M_{1+})$ at the resonance pole.

Extraction of $\sigma_{LT'}$ was made through a measurement of the electron beam asymmetry $A_{LT'}$:

$$A_{LT'} = \frac{d^2\sigma^+ - d^2\sigma^-}{d^2\sigma^+ + d^2\sigma^-} \quad (5)$$

$$= \frac{\sqrt{2\epsilon_L(1-\epsilon)}\sigma_{LT'}\sin\theta_\pi^*\sin\phi_\pi^*}{\sigma_0}. \quad (6)$$

$A_{LT'}$ was obtained by dividing the measured asymmetry A_m by the magnitude of the electron beam polarization P_e :

$$A_{LT'} = \frac{A_m}{P_e}, \quad (7)$$

$$A_m = \frac{N_\pi^+ - N_\pi^-}{N_\pi^+ + N_\pi^-}, \quad (8)$$

where N_π^\pm is the number of π^0 events per incident electron for each electron beam helicity state. $A_{LT'}$ was determined for individual bins of $(Q^2, W, \cos\theta_\pi^*, \phi_\pi^*)$. Normalization factors cancel in Eq. (6), and since acceptance studies showed no significant helicity or bin size dependence, acceptance factors canceled in A_m as well. This leaves A_m largely free from systematic errors. Radiative corrections were applied for each bin using the program recently developed by Afanasev *et al.* for exclusive pion electroproduction [20]. Cor-

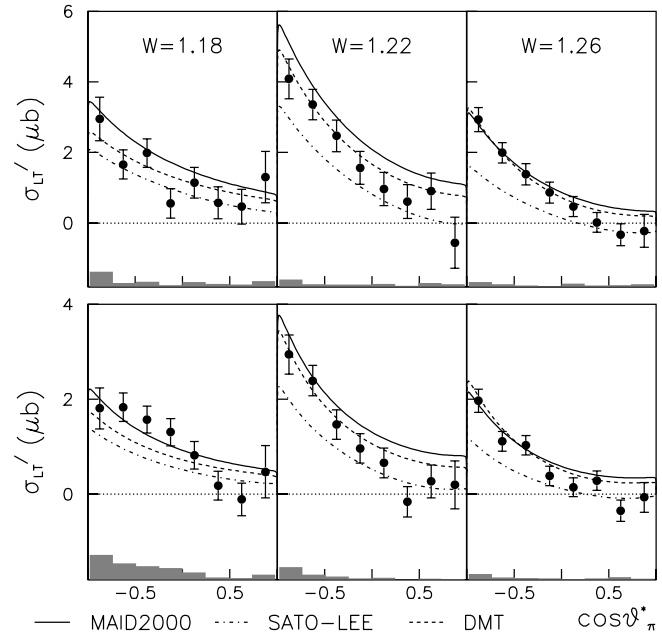


FIG. 1. CLAS measurement (\bullet) of $\sigma_{LT'}$ vs $\cos\theta_\pi^*$ extracted at $Q^2=0.40$ GeV 2 (top) and $Q^2=0.65$ GeV 2 (bottom). Curves show model predictions. Shaded bars show systematic errors.

rections were also applied to compensate for cross section variations over the width of each bin. The corrected $A_{LT'}$ was multiplied by the unpolarized cross section σ_0 . A parametrization of σ_0 was used, which was obtained from the SAID PR01 solution [21] fitted to previously measured CLAS data and world data. The structure function $\sigma_{LT'}$ was then extracted using Eq. (6) by fitting the ϕ_π^* distributions. Systematic errors for $\sigma_{LT'}$ were dominated by uncertainties in determination of the electron beam polarization and the parametrized unpolarized cross section σ_0 . The systematic error for A_m is negligible in comparison. Quadratic addition of the individual contributions yields a total relative systematic error of $<6\%$.

Figure 1 shows $\sigma_{LT'}$ extracted at $Q^2=0.40$ GeV 2 and $Q^2=0.65$ GeV 2 , where the $\cos\theta_\pi^*$ dependence is plotted for W bins of 1.18, 1.22, and 1.26 GeV. The measured angular distributions show a strong backward peaking for W bins around the $\Delta(1232)$ mass. The curves show predictions from recent models [10,22,23] which use different methods to satisfy unitarity in the $\pi^0 p$ final state. These models, which are fitted to previous photoproduction and unpolarized electroproduction data, include backgrounds arising from Born diagrams and t -channel vector meson exchange. The Sato-Lee [10] and Dubna-Mainz-Taipei [22] (DMT) models use an off-shell πN reaction theory to calculate unitarity corrections, while the more phenomenological MAID2000 model [23] incorporates πN phases directly into the background amplitudes. While the models describe the data qualitatively, none of the calculations is able to describe both the overall magnitude and the slope of the measured c.m. angular distributions consistently.

A more quantitative comparison was made through fitting the extracted $\sigma_{LT'}$ angular distributions using the Legendre expansion:

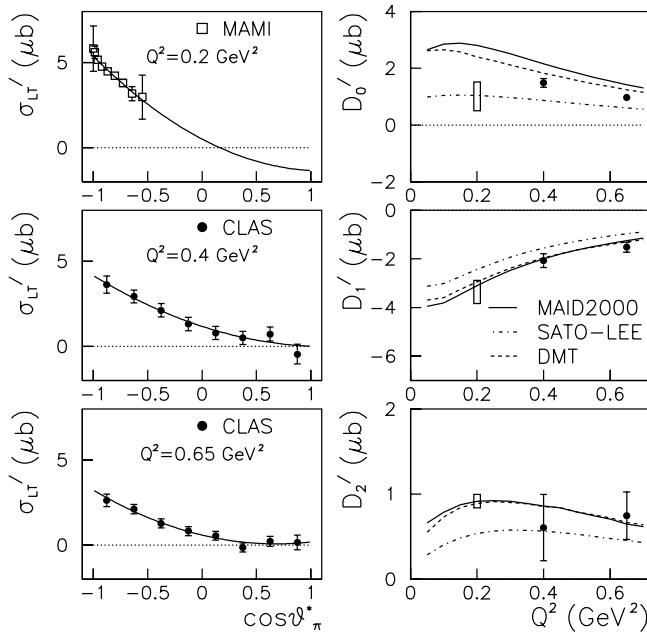


FIG. 2. Left: Fits to $\sigma_{LT'}$ angular distributions measured by CLAS (middle, bottom) and MAMI (top) at $W=1232$ GeV using Eq. (9). See text for details. Right: Q^2 dependence of Legendre moments of $\sigma_{LT'}$. Curves show model predictions. Data points are the present CLAS measurement. Vertical bars at $Q^2=0.2$ GeV 2 show moments obtained from model constrained fits to MAMI data [16].

$$\sigma_{LT'} = D'_0 + D'_1 P_1(\cos \theta_\pi^*) + D'_2 P_2(\cos \theta_\pi^*), \quad (9)$$

where $P_l(\cos \theta_\pi^*)$ is the l th-order Legendre polynomial and D'_l is the corresponding Legendre moment. Each moment can be decomposed into interference terms involving the leading-order magnetic ($M_{l_\pi^\pm}$), electric ($E_{l_\pi^\pm}$), and scalar ($S_{l_\pi^\pm}$) multipoles:

$$D'_0 = -\text{Im}[(M_{1-} - M_{1+} + 3E_{1+})^* S_{0+} + E_{0+}^* (S_{1-} - 2S_{1+}) + \dots] \quad (10)$$

$$D'_1 = -6 \text{Im}[(M_{1-} - M_{1+} + E_{1+})^* S_{1+} + E_{1+}^* S_{1-} + \dots] \quad (11)$$

$$D'_2 = -12 \text{Im}[(M_{2-} - E_{2-})^* S_{1+} + 2E_{1+}^* S_{2-} + \dots], \quad (12)$$

where l_π is the $\pi^0 p$ angular momentum whose coupling with the nucleon spin is indicated by \pm .

Figure 2 shows typical fits to $\sigma_{LT'}$ angular distributions near the peak of the $\Delta(1232)$ resonance (left), while the Q^2 dependence of the extracted Legendre moments is compared to model predictions (right). The largest disagreement with models clearly occurs for D'_0 , which is dominated by interference terms involving s -wave πN multipoles. The CLAS data also require $D'_2 \neq 0$. The fitted D'_2 strength has the same sign and overall magnitude as the model predictions, although we cannot differentiate between the models due to

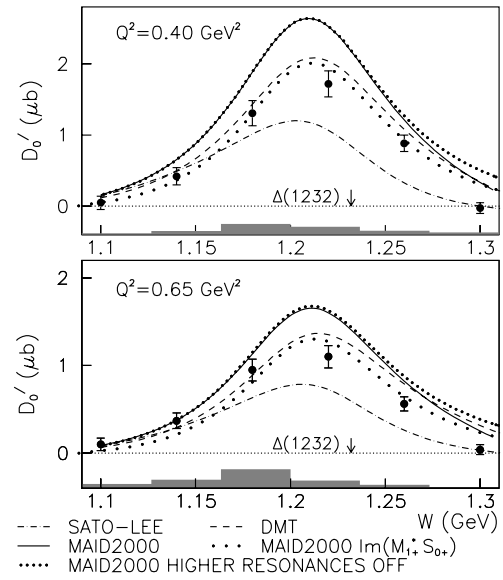


FIG. 3. CLAS measurement (\bullet) of Legendre moment D'_0 vs W (GeV). Curves show recent model calculations that include contributions from multipoles up to angular momentum $l_\pi=5$. Shaded bars show systematic errors.

large statistical uncertainties. No evidence for d waves was observed in our measurement of σ_{LT} [1].

We also compare our fit results with a recent MAMI measurement [16] of the beam asymmetry $A_{LT'}$ at $Q^2 = 0.2$ GeV 2 . The published MAMI angular distribution was converted to $\sigma_{LT'}$ using Eq. (6) and MAID2000 for the unpolarized cross section σ_0 . Since the MAMI data do not have sufficient angular coverage to determine D'_2 , the fit was performed by constraining D'_2 relative to D'_1 using MAID2000. With D'_2 fixed, the remaining Legendre moments estimated from the MAMI data can be compared to the Q^2 trend of the CLAS data (Fig. 2, right). Both datasets suggest an anomalous behavior for D'_0 with respect to the models. However, a recent Bates measurement [17] of $\sigma_{LT'}$ at $Q^2 = 0.127$ GeV 2 and $\theta_\pi^* = 129^\circ$ found good agreement with MAID2000 and DMT, although no angular distributions were reported.

Figures 3 and 4 show the W dependence of the fitted Legendre moments, D'_0 and D'_1 , respectively. Both moments show strong resonant behavior, suggesting dominance of interference terms involving the multipoles of the $\Delta(1232)$. Our measurement of D'_0 is substantially below the predictions of MAID2000, and in closer agreement with the DMT dynamical model at $W=1.18$ GeV, while the Sato-Lee prediction is smaller still. For increasing W , our data fall below the DMT curve, while none of the models describes the W dependence well. Note that contributions of higher resonances to D'_0 are negligible except near $W=1.30$ GeV. Figure 4 shows the fit results for D'_1 . Here our comparison with models shows some Q^2 dependence. Better agreement with the dynamical models occurs below the $\Delta(1232)$ at $Q^2 = 0.4$ GeV 2 , while at $Q^2 = 0.65$ GeV 2 all of the W points are systematically larger than the predictions.

The large differences between the model predictions for

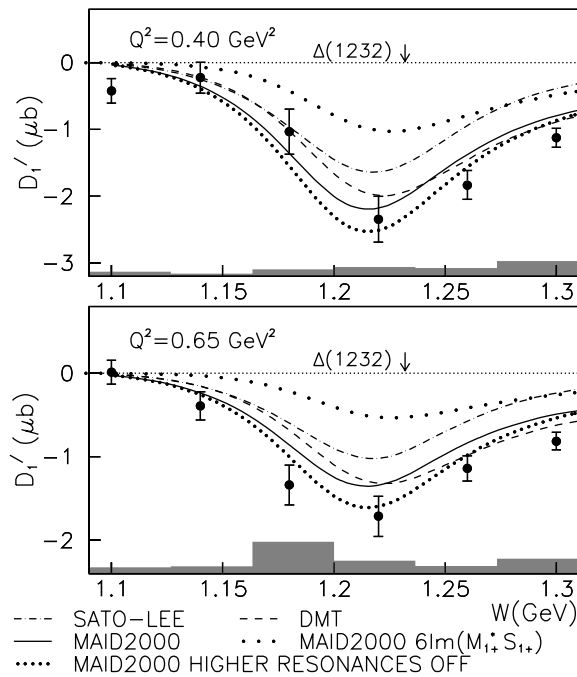


FIG. 4. CLAS measurement (●) of Legendre moment D'_1 vs W (GeV). See Fig. 3 for details.

D'_0 arise from the term $\text{Im}(M_{1+}^* S_{0+})$, which produces 70%–75% of the total strength in MAID2000. In contrast, D'_1 is more sensitive to higher resonances, which contribute 15%–20% in MAID2000 [coming mainly from $\text{Im}(M_{1+}^* S_{1+})$], while $\text{Im}(M_{1+}^* S_{1+})$ accounts for $\approx 40\%$ of the total strength. The S_{0+} multipole is an important background affecting the

extraction of the $\gamma^* p \rightarrow \Delta(1232)$ $C2$ Coulomb quadrupole transition, and is sensitive to choices of πNN coupling and contributions from final state πN rescattering [23]. Unfortunately, a simple rescaling of the S_{0+} strength, as suggested in Ref. [16], is not sufficient to account for the inferred Q^2 dependence of D'_0 .

In summary, complete angular distributions for the polarized structure function $\sigma_{LT'}$ were measured for the first time, using the $p(\vec{e}, e' p)\pi^0$ reaction. In accordance with measurements at lower Q^2 [14–17], evidence for significant nonresonant background in the $\Delta(1232)$ region is seen. A departure from the predicted Q^2 dependence of various effective Lagrangian based models is seen at the $\Delta(1232)$ peak when the CLAS data are compared to the MAMI data at $Q^2 = 0.2$ GeV². Examination of the Legendre moments D'_0 and D'_1 shows the discrepancies are largest for D'_0 . CLAS measurements in the Q^2 range of 0.1–0.4 GeV² and also for $W > 1.3$ GeV are currently being analyzed to provide more information on the form factors of the underlying multipoles.

We acknowledge the efforts of the staff of the Accelerator and Physics Divisions at Jefferson Lab in their support of this experiment. This work was supported in part by the U.S. Department of Energy and National Science Foundation, the Emmy Noether Grant from the Deutsche Forschungsgemeinschaft, the French Commissariat à l'Énergie Atomique, the Italian Istituto Nazionale di Fisica Nucleare, and the Korea Research Foundation. The Southeastern Universities Research Association (SURA) operates the Thomas Jefferson Accelerator Facility for the U.S. Department of Energy under Contract No. DE-AC05-84ER40150.

- [1] K. Joo *et al.*, Phys. Rev. Lett. **88**, 122001 (2002).
 [2] C. Mertz *et al.*, Phys. Rev. Lett. **86**, 2963 (2001).
 [3] V.V. Frolov *et al.*, Phys. Rev. Lett. **82**, 45 (1999).
 [4] K. Bermuth *et al.*, Phys. Rev. D **37**, 89 (1988).
 [5] H. Walliser and G. Holzwarth, Z. Phys. A **357**, 317 (1997).
 [6] A. Silva *et al.*, Nucl. Phys. **A675**, 637 (2000).
 [7] L. Amoreira, P. Alberto, and M. Fiolhais, Phys. Rev. C **62**, 045202 (2000).
 [8] S. Capstick and G. Karl, Phys. Rev. D **41**, 2767 (1990).
 [9] N. Isgur, G. Karl, and R. Koniuk, Phys. Rev. D **25**, 2394 (1982).
 [10] T. Sato and T.-S.H. Lee, Phys. Rev. C **63**, 055201 (2001).
 [11] S.S. Kamalov *et al.*, Phys. Rev. C **64**, 032201(R) (2001).
 [12] G. Gellas *et al.*, Phys. Rev. D **60**, 054022 (1999).
 [13] C. Alexandrou *et al.*, hep-lat/0307018.
 [14] T. Pospischil *et al.*, Phys. Rev. Lett. **86**, 2959 (2001).
 [15] G. Warren *et al.*, Phys. Rev. C **58**, 3722 (1998).
 [16] P. Bartsch *et al.*, Phys. Rev. Lett. **88**, 142001 (2002).
 [17] C. Kunz *et al.*, Phys. Lett. B **564**, 21 (2003).
 [18] N.F. Sparveris *et al.*, Phys. Rev. C **67**, 058201 (2003).
 [19] B. Mecking *et al.*, Nucl. Instrum. Methods. A **503**, 513 (2003).
 [20] A. Afanasev, I. Akushevich, V. Burkert, and K. Joo, Phys. Rev. D **66**, 074004 (2002).
 [21] R. Arndt, W. Briscoe, I. Strakovsky, and R. Workman, nucl-th/0301068.
 [22] S.S. Kamalov and S.N. Yang, Phys. Rev. Lett. **83**, 4494 (1999).
 [23] D. Drechsel *et al.*, Nucl. Phys. **A645**, 145 (1999), see www.kph.uni-mainz.de/MAID/